D. V. Giri
Y. Rahmat-Samii
1 May 1992

Microwave Memos
Memo 6

Mark 0 Phaser

I. Introduction

Various considerations in the design of a possible high-power microwave (HPM) weapon (phaser) have been addressed in the past [1 to 14]. The term "phaser" stands for pulsed high-amplitude sinusoidal electromagnetic radiation. A progression of potential phaser designs referred to as "Mark N Phaser" was conceptualized in [14]. This class of phasers is defined by

$$P_s \simeq 10^N \text{ in } GW \tag{1}$$

where P_s is the useful power. This definition is useful at a nominal frequency of about 1 GHz. Adjustments for lowered power levels at higher frequencies can be made, if needed. Useful power from an HPM source is the power in the lowest order mode of a waveguide (e.g., the $H_{1,0}$ mode of a standard rectangular waveguide) with an operating frequency below the cut off frequencies of other modes, or a set of such waveguides with controlled phase relationship among them.

The objective of this memo is to describe in detail the design considerations of a Mark 0 Phaser. It is emphasized that we are concerned with single-shot operation of the phaser with the purpose of damaging or causing a functional upset of the target system. Phasers are not necessarily intended to destroy the target, but deny a successful mission. Given that semiconductor devices are physically small and only take about a microsecond to dissipate heat, microwave weapons that maximize the burn-out threat for a given source energy would be pulsed devices with pulse widths of the order of a microsecond or less. Phasers operating in a single shot mode are very appropriate and relevant. It can be argued that a single pulse with relatively large power is more damaging to the target than a repetitive HPM source with smaller power at repetitive rates of kHz or less. The repetitive HPM sources may have other application such as a high-power jammer in electronic warfare.

II. Mark 0 Phaser at ~1 GHz

The Mark 0 Phaser described here is a 1.1 GHz; 1 GW average power; 100 ns pulse duration, system that can readily be assembled. A relativistic magnetron source is commercially available [15] with the following capability

---

This work was performed jointly by Dr. D. V. Giri (Pro-Tech) and Prof. Y. Rahmat-Samii (UCLA) and was sponsored by the U. S. Army. The authors are thankful to Dr. Carl Baum of Phillips Laboratory for valuable discussions.

frequency	=	1.1 GHz	
wavelength	=	0.2727 m	
period	=	0.909 ns	
peak power	=	1.8 GW	
average power	=	0.9 GW	; single shot operation
waveguide	=	WR - 650	; a = 0.1651 m , b = 8.25 cm
pulse width	=	60 ns	; contains 66 cycles

It should be possible to make the appropriate modifications to this commercially available source as follows

i) obtain a peak power of 2 GW, corresponding to an average power of 1 GW

ii) use WR-975 waveguide instead of WR-650

iii) increase the pulse width from 60 ns to 100 ns.

The above modifications are required for the following reasons.

a) One can increase the power level by about 10% to more closely correspond to Mark 0 Phaser requirement. We are of course referring to useful power carried in the dominant mode of a rectangular waveguide. This could be an optional modification since the available useful power is only 10% below the level of 1 GW, for a Mark 0 Phaser.

b) The use of WR-975 rectangular waveguide is preferred so that eventual upgrading to higher power levels is relatively easier. The WR-650 presently used with this source are useful for $H_{1,0}$ operation in the frequency range of 1.1 to 1.7 GHz as listed. The cut off frequency of $H_{1,0}$ mode for WR-650 waveguide is 908 MHz, where as for the WR-975, it is 605.69 MHz. The next higher cut off frequency ($H_{0,1}$ & $H_{2,0}$) in WR-975 is at 1.2114 GHz, which is ~10% higher than the operating frequency of 1.1 GHz. Consequently, WR-975 is the optimal waveguide in terms of power handling capacity at 1.1 GHz operation.

c) A pulse width of 100 ns will contain about 110 cycles and from an interaction viewpoint, ~100 cycles should be adequate to ring up most system resonances [11] resulting in the maximum signal (voltage or current) at the failure port. From an energy or fluence point of view, the incident energy at the target will increase with pulse width for a fixed peak power from the source, and some special target classes may call for longer pulse widths.

A. Rectangular waveguides

Now that we have identified a commercially available relativistic magnetron source, the next element is the rectangular waveguide in terms of how many and the field levels inside. It is clearly possible to carry all of this useful power of 1 GW (average) in a single WR-975 waveguide.

A peak power of 1.8 GW has already been carried by a WR-650 waveguide in the dominant mode of propagation [15]. The corresponding peak electric field in the waveguide is given by [9]

$$E_{peak} = \sqrt{\frac{2P_{peak}Z_{1,0}}{ab}} \tag{2}$$

where $Z_{1,0}$ is the $H_{1,0}$ modal impedance given by

$$Z_{1,0} = Z_0\left[1 - \left(\frac{\lambda}{2a}\right)^2\right]^{-1/2} \tag{3}$$

Substituting $Z_0 = 376.98\ \Omega$, $\lambda = 0.273$ m, $a = 165.1$ mm for the WR-650 waveguide, we have $Z_{1,0} \simeq 670.8\ \Omega$. Using this value of $Z_{1,0}$, $P_{peak} = 1.8$ GW, $a = 0.1651$ m, $b = 0.0825$ m we get

$$E_{peak}(WR-650) \simeq 13.32\ MV/m \tag{4}$$

which has been sustained without breakdown. Assume that the above source, along with its waveguide extraction is upgraded to $P_{peak} = 2$ GW using a single WR-975 waveguide. The inner dimensions of WR-975 are a = 247.65 mm and b = 123.83 mm and the $H_{1,0}$ modal impedance is 473.8 Ω [9]. This results in a peak field of

$$E_{peak}(WR-975) = \sqrt{\frac{2P_{peak}Z_{1,0}}{ab}}$$

$$= \sqrt{\frac{2\times2\times10^9\times473.8}{0.24765\times0.12383}} = 7.86MV/m \tag{5}$$

Clearly, this can be sustained without breakdown, in comparison with (4). The advantage of changing the waveguide from WR-650 to WR-975 is also obvious. The use of WR-975 can lead to much higher power handling capability. It should also be pointed out that in the event that the 2 GW peak power is extracted from the source in more than one WR-975 waveguide, it is possible to combine waveguide [5], so that eventually all of the power is carried by a single WR-975 waveguide.

B. Waveguide flanges

The need is for "vacuum flanges," since the waveguides are evacuated. The vacuum levels are typically ~10^{-6} mm of Hg in the waveguides and about 3×10^{-7} mm Hg in the source (e.g., anode-cathode region of a relativistic magnetron) [15]. The requirements of vacuum pumps are governed by such levels.

C. Sidewall bidirectional couplers

Since the side wall or the H-wall is a charge free surface for the $H_{1,0}$ mode, it is the preferred wall for coupling a portion of the forward and reflected power for measurement. Design equations and charts are available for side wall couplers [16]. As an example, results for a two-hole, side wall coupler are available in [16]. The design curve on page 8 of [16] is for the case of both the main and secondary guides with aspect ratio a:b of 2:1, which is the case for WR-975 waveguides. An illustrative design for a sidewall coupler, with about a 50 dB coupling is listed in Table 1.

TABLE 1. Illustrative example of a side wall coupler

waveguide WR-975 ; f = 1.1 GHz ; λ = 27.27 cm

a = 247.65 mm = 2b => aspect ratio 2:1

d = diameter of 2 circular holes in the H-wall

(d/a) = 0.15 => d = 37.15 mm

s ≡ separation between the 2 holes = $\lambda_g/4$

$$\lambda_g = \lambda\left[1 - \left[\frac{\lambda}{2a}\right]\right]^{-1/2} = 32.7cm$$

$$s = \frac{\lambda_g}{4} = 81.75 \text{ mm}$$

50 dB ≤ coupling ≤ 55 dB

In the above table, the coupling is shown to be 50 to 55 dB over the low to high frequency band. A 90 dB coupler would sample 1 Watt from 1 GW. Such a 90 dB coupler can be made up of two 45 dB couplers or a combination of 50 dB and 40 dB couplers. The equations and design curves in [16] may be used in fabricating the required H-wall couplers.

An important criterion in the design of a directional coupler is the directivity or the front to back ratio. It is the difference between the desired and undesired couplings. If a coupler has low directivity, the forward and reverse powers in the coupler interface leading to inaccuracies in measurement. One could investigate the use of a sidewall coupler with many holes, in obtaining an improved directivity that can be maintained over a broader band of frequencies. The design equations for a many-hole side wall coupler are also well established and available [16].

D. Feed horn

The pyramidal horn along with its two dielectric interfaces i.e., vacuum to SF_6 at 1 atmosphere and SF_6 to outside air is schematically shown in figure 1. With reference to figure 1, the peak electric field at the horn-exit aperture is estimated by

$$E_{peak}(\text{horn-exit}) = E_{peak}(\text{waveguide})\sqrt{\frac{ab}{a'b'}}$$

$$= E_{peak}(\text{waveguide})\left[\frac{b}{b'}\right] \quad \text{if} \quad \left[\frac{a}{b} = \frac{a'}{b'}\right] \tag{6}$$

Substituting a waveguide field of 7.86 MV/m, it is seen that $(b/b') \leq 0.382$ or $(b'/b) \geq 2.62$ in order that the peak electric field at the horn-exit aperture is ≤ 3 MV/m. This ensures a safe transition from vacuum to SF_6 (1 atmosphere) medium at the horn exit. This corresponds to a minimum length of a pyramidal

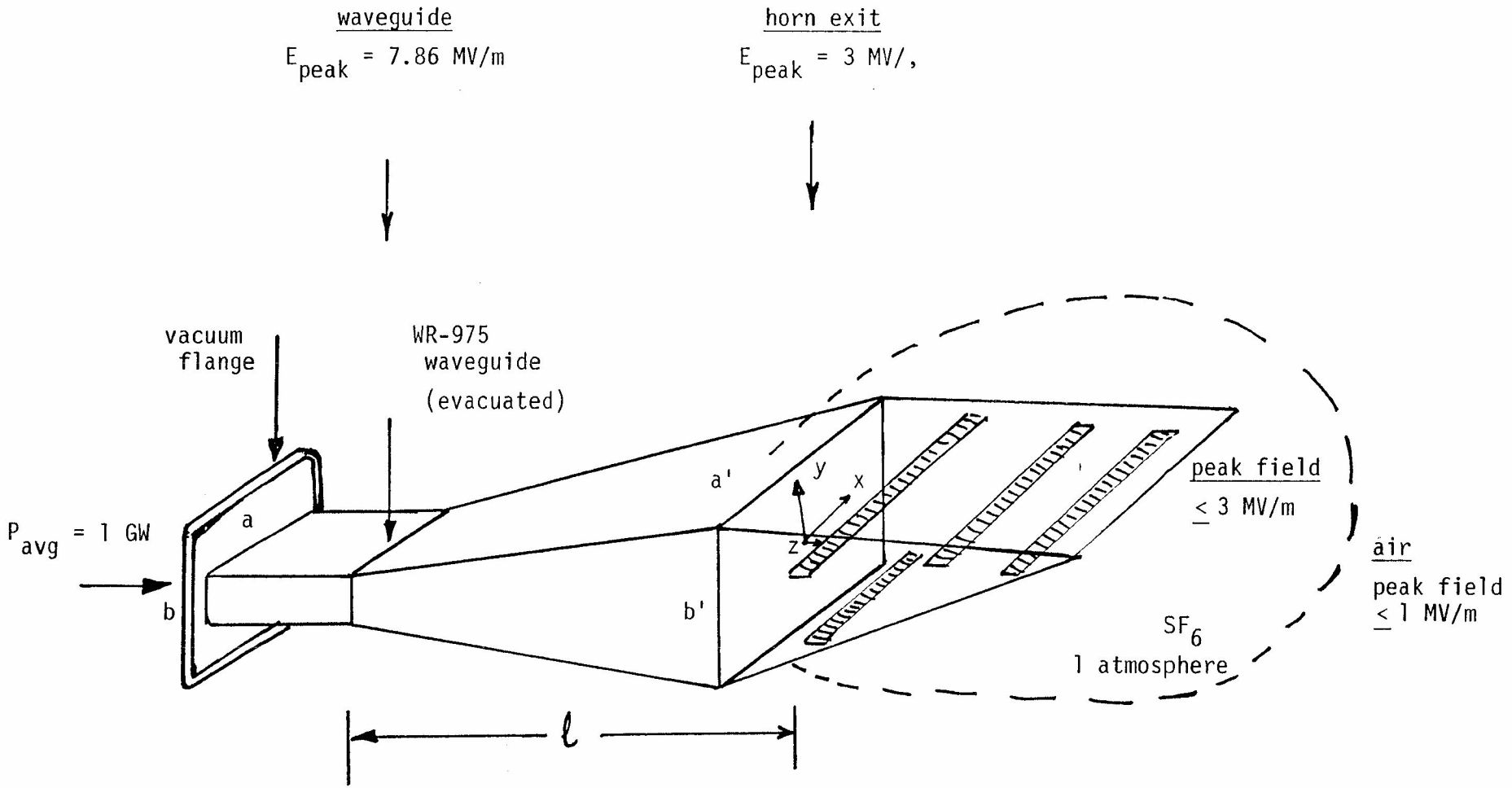

Figure 1. Feed horn for Mark 0 Phaser.

horn, for chosen flare angles. Some of the dimensions of the feed horn are listed in Table 2.

TABLE 2. Dimensions of the Waveguide and Feed Horn

WR-975 waveguide	Pyramidal feed horn	
a = 24.765 cm	$a' \geq$ 64.884 cm	
b = 12.383 cm	$b' \geq$ 32.443 cm	f = 1.1 GHz λ = 27.27 cm
a/λ = 0.908	$a'/\lambda \geq$ 2.38	
b/λ = 0.454	$b'/\lambda \geq$ 1.190	

when the equality sign holds, the field at the horn-exit is about 3 MV/m which is acceptable for transitioning from vacuum to SF_6 at 1 atmosphere. This pyramidal horn assumes equal E-plane and H-plane flare angles when the equality holds, resulting in a horn-exit aperture area of 2.832 λ^2 = 0.211 m^2. The peak electric field at the horn-exit aperture may also be verified from the power consideration as

$$E_{peak}(horn-exit) = \sqrt{\frac{2 \times P_{peak} \times Z_{1,0}}{a'b'}}$$

$$= \sqrt{\frac{2 \times 2 \times 10^9 \times 473.8}{0.211}} \simeq 3\,MV/m \qquad (7)$$

Of course, it is not essential that the two flare angles be the same (i.e., a:a' :: b:b'). Other horn geometries may be desirable to better illuminate the reflector, as was considered in [13].

Two examples are worked out in detail, later in this memo. They consist of an offset fed circular and elliptical reflectors.

E. Dielectric interface

In order to specify the axial length of the polyethelene bag attached to the horn aperture, we can simply use the analytical expression for the Fresnel electric field on axis, given by [8] as

$$E_y(0,0,z) \simeq \frac{E_0}{2} \frac{\ell_E \ell_H}{(\ell_E + z)(\ell_H + z)} F_1(u)\ F_2(v) \qquad (8)$$

Equation (8) above is the same as (4.18 of [8]) where all of the parameters and functions are defined. E_0 in (8) corresponds to the peak electric field at the horn exit aperture, which has been constrained to be $\leq$ 3 MV/m. It is easy enough to find a distance "z" in (8), where the field has dropped to $\leq$ 1 MV/m on axis, so that one can transition from SF_6 at 1 atmosphere to outside air. This calculation will give adequate details for the minimum size of the polyethelene bag that holds SF_6 at 1 atmosphere. The length of the wedge shaped dielectric interface could then be suitably scaled.

F. Offset parabolic reflector antenna

As before [9], we may consider aperture areas for the parabolic reflector to be 20 m^2, 40 m^2 and 100 m^2. Of these three choices, the smallest one with the aperture area of about 20 m^2 is truck mountable as sketched in figures 2 and 3. The difference between the two is the shape of the radiating aperture, circular in figure 2 and elliptical in figure 3. In the case of figure 2, the reflector could be normally folded in the middle and opened out during use. Of the two choices, the circular aperture can produce both horizontal and vertical polarization of the electric field by a rotation of the feed horn and may be preferable for this reason. The field at the circular reflector of diameter D, scales approximately as,

$$E_{\text{reflector}} = E_{\text{waveguide}} \times \frac{b}{D}$$

$$= 7.86\left[\frac{MV}{m}\right] \times \frac{0.123m}{5m} \simeq 193\ kV/m \tag{9}$$

Assuming a uniform illumination of the reflector (not quite the case), we can estimate the far field as follows

$$E_{peak}(\text{far field}) = E_{\text{reflector}}\left[\frac{A}{R\lambda}\right]\ V/m \tag{10}$$

$$p_{avg}(\text{far field}) = \left[\frac{E^2_{peak}(\text{far field})}{2Z_0}\right]\ W/m^2 \tag{11}$$

$$\text{energy density} \equiv \text{fluence} \equiv u = p_{avg}\Delta t\ \ J/m^2 \tag{12}$$

For $E_{reflector} \simeq$ 193 kV/m , A = 20 m^2, λ = 27.27 cm and Δt = 100 ns, we get the following far field characteristics.

TABLE 3. Far Field Characteristics of Mark 0 Phaser at 1.1 GHz with 20 m^2 radiating aperture

R km	E_{peak} (far field) kV/M	p_{avg} (far) kW/m^2	fluence U J/m^2
1	14	260	2.6×10^{-2}
3	4.67	29	2.9×10^{-3}
10	1.4	2.6	2.6×10^{-4}
20	0.7	0.65	0.65×10^{-4}

We defer the discussion of these results, to a later section of this memo. Some of the issues relating to the

NOT TO SCALE

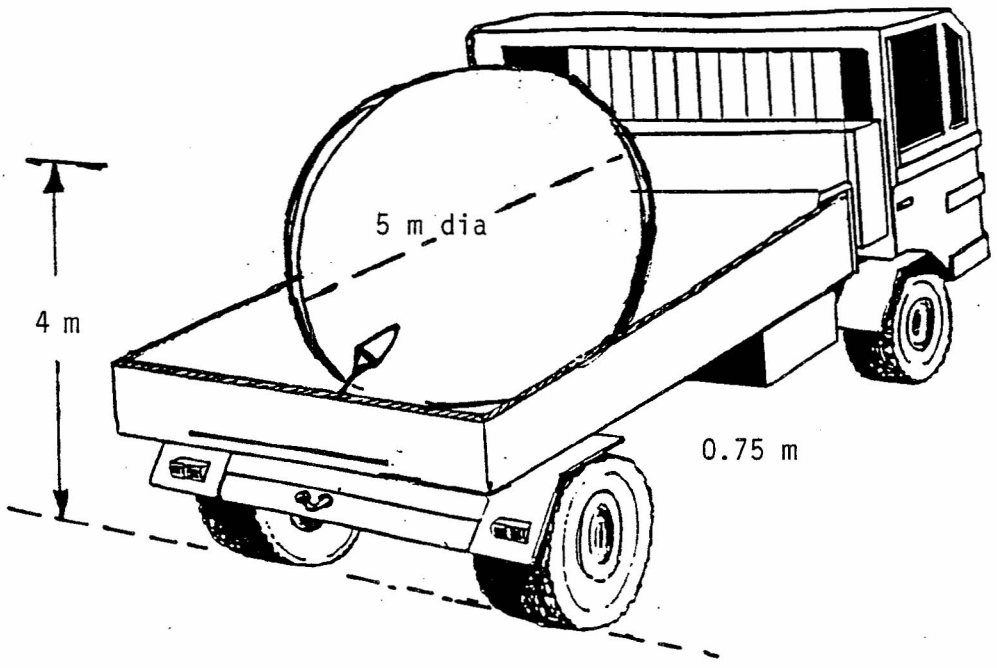

Figure 2. Truck mounted offset fed circular reflector; 5 m dia. and paraboloidal surface with an area of ~19.6 m^2.

NOT TO SCALE

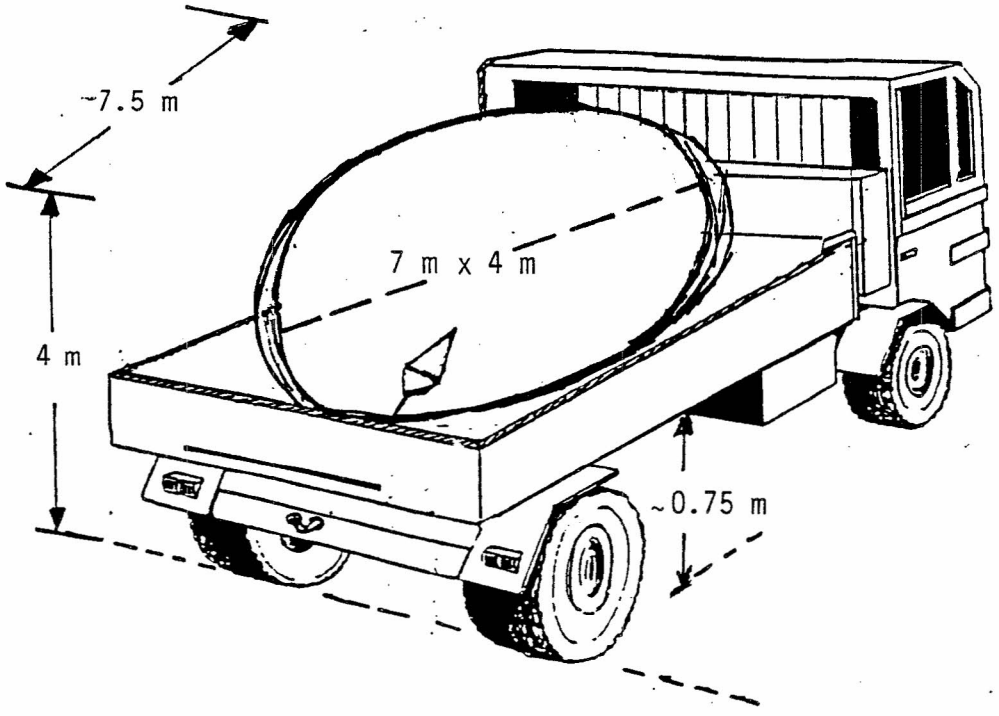

Figure 3. Truck mounted offset fed elliptical reflector; with an area of ~21.9 m^2.

transportability and power requirements of such an antenna system that need to be addressed in future studies are:

a) an arrangement to fold the antenna in the middle during the transport,

b) explore the feasibility of employing evacuated flexible waveguides,

c) placing the reflector on a rotatable platform,

d) power requirements for the source and vacuum systems from a diesel powered generator that could be in a trailer or accompanying truck,

e) shielding requirements for the electronic components or systems in the source and the truck.

G. Illustrative examples

In this subsection, we have worked out the detailed geometries of two possible single reflector antenna geometries that are truck-mountable as sketched in figures 2 and 3.

Example 1. Circular reflector with a diameter = 5m; A = 19.63 m^2

Example 2. Elliptical reflector with major and minor axes of 7 m and 4 m; A = 21.99 m^2.

and these are described below

Example 1: Circular reflector

An optimal pyramidal horn feed has been worked out, to illuminate the circular reflector. The feed and reflector geometries are shown in figure 4, the radiation patterns of the horn illuminating the circular reflector are shown in figures 5 and the far field patterns of the reflector antenna are shown in figure 6.

The actual field strengths are calculated for the circular reflector at a few typical distances. The results are shown in Table 4.

TABLE 4: Far Field Parameters of the Circular Reflector Antenna

R km	E_{peak} (far field) kV/M	p_{avg} (far) kW/m^2	fluence U J/m^2
1	12.8	220	2.2×10^{-2}
3	4.3	24	2.4×10^{-3}
10	1.3	2.2	2.2×10^{-4}
20	0.64	0.54	0.5×10^{-4}

A comparison of the results in Table 4 with the estimated values (assuming a 100% antenna efficiency) in Table 3 shows that the fluence levels produced by the circular reflector is about 72% of the estimates in Table 3.

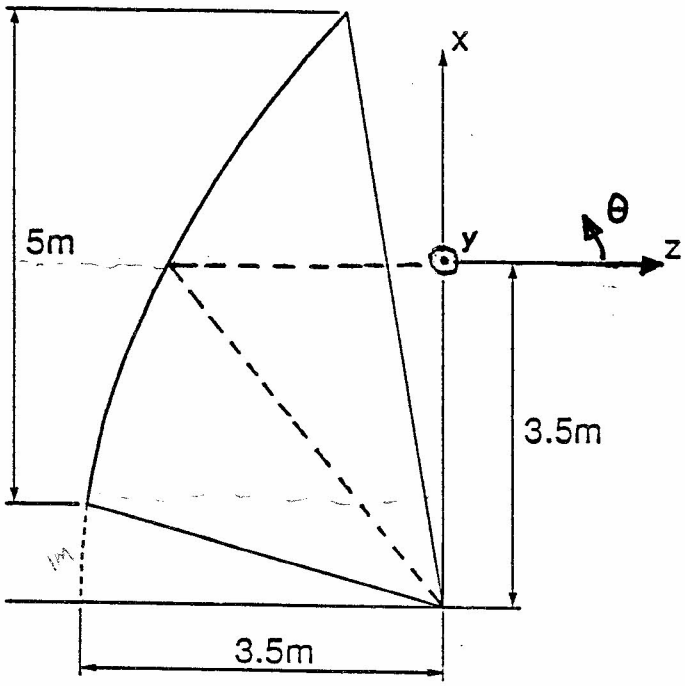

(a) reflector geometry with an offset feed

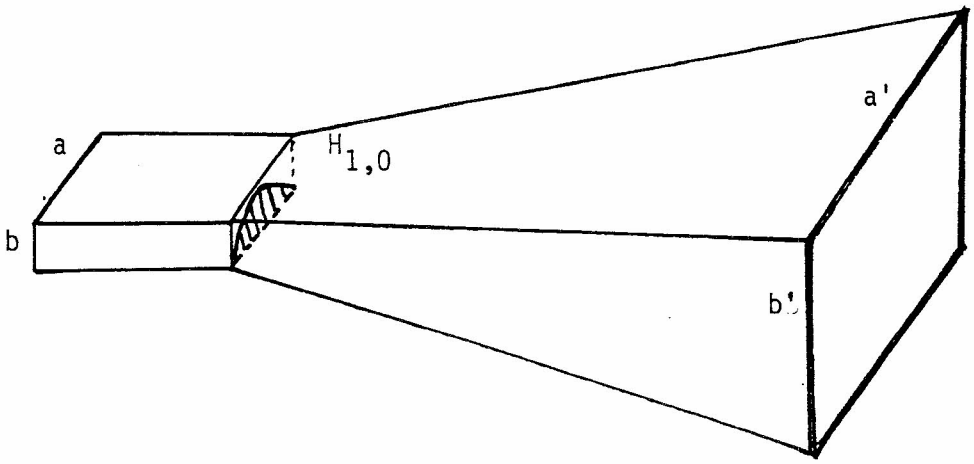

a = 0.247 m
b = 0.123 m
a' = 0.565 m
b' = 0.413 m
= 1.371 m

flare angles

H-plane = 6.61^{o}
E-plane = 6.03^{o}

(b) dimensions of the feed horn (not to scale)

Figure 4. An offset fed circular reflector (example 1)

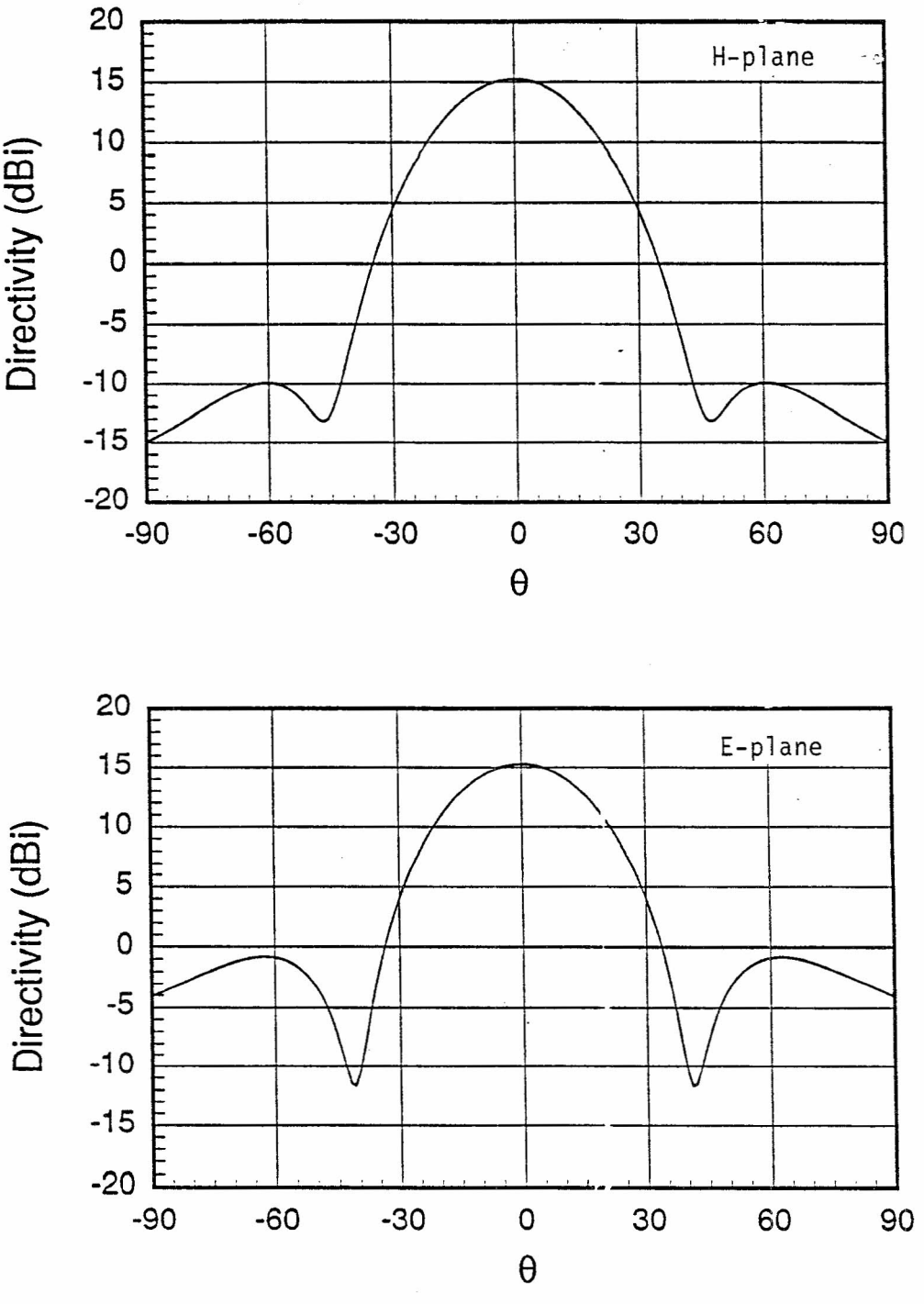

Figure 5. Radiation patterns of the pyramidal horn in figure 4.

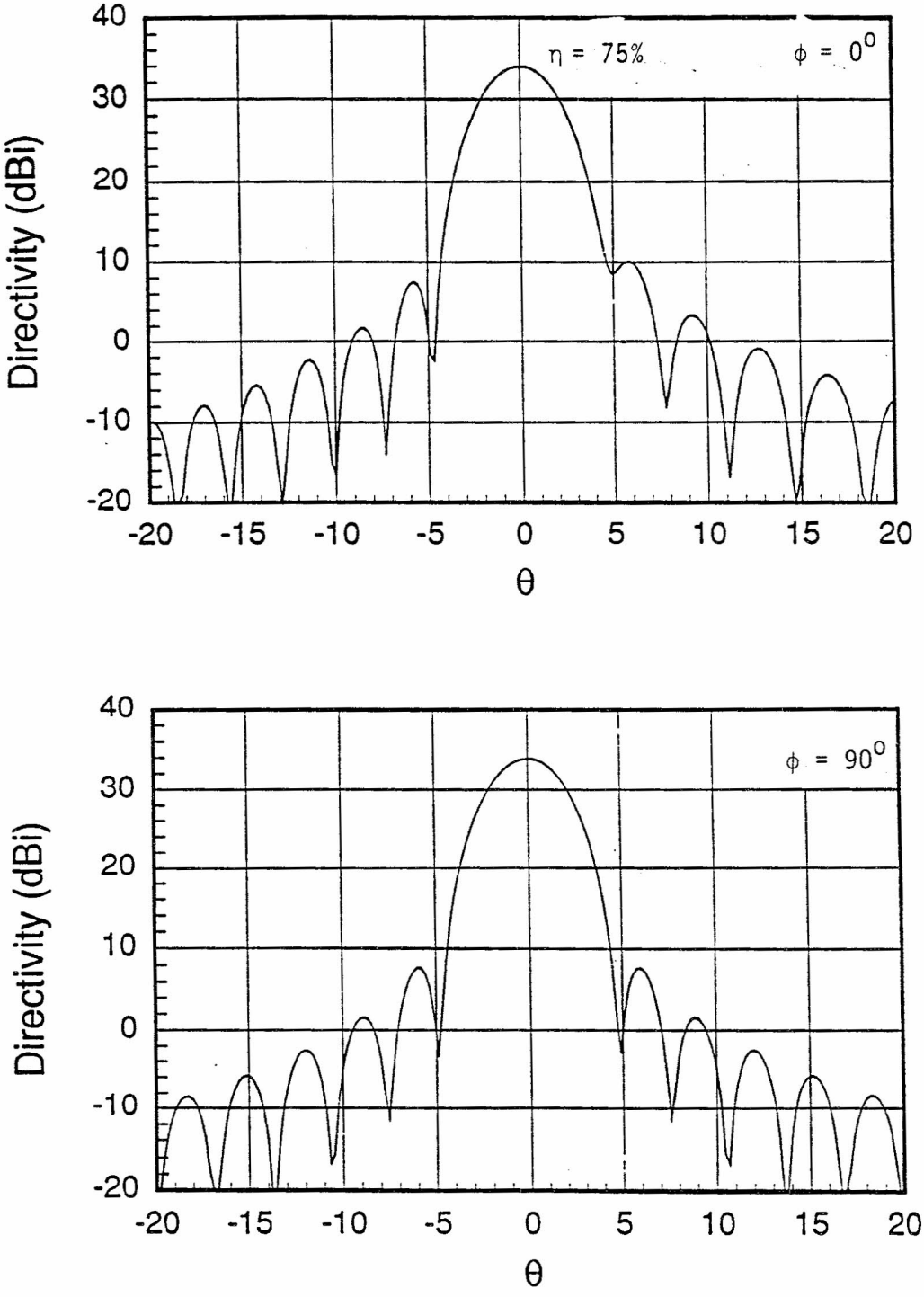

Figure 6. Radiation patterns of the circular aperture at 1.1 GHz.

Example 2: Elliptical reflector

An optimal pyramidal horn feed has been worked out, to illuminate the elliptical reflector, the feed and reflector geometries are shown in figure 7, the radiation patterns of the horn, illuminating the elliptical reflector are shown in figure 8 and the far field patterns of the reflector antenna are shown in figure 9.

Once again the actual field strengths are calculated for the elliptical reflector at a few typical distances. The results are shown in Table 5.

TABLE 5: Far field parameters of the elliptical reflector antenna

R km	E_{peak} (far field) kV/m	p_{avg} (far) kW/m^2	fluence U J/m^2
1	11.9	190	1.9×10^{-2}
3	4.0	21	2.1×10^{-3}
10	1.2	1.9	1.9×10^{-4}
20	0.60	0.48	0.5×10^{-4}

A comparison of the results in Table 5 with the estimated values (assuming a 100% antenna efficiency) in Table 3 shows that the fluence levels produced by the circular reflector is about72% of the estimates in Table 3.

It is also noted that in the elliptical reflector example, the electric field is polarized along the minor axis of the ellipse. If the orthogonal polarization i.e., electric field parallel to the major axis of the ellipse is desired, the horn design can easily be altered for optimal performance.

In the next section, we briefly discuss a Mark 0 Phaser at a frequency of 2.8 GHz.

III. Mark 0 Phaser at 2.8 GHz

The design parameters and the far field characteristics of the Mark 0 Phaser at this higher frequency may be summarized as follows. The frequency of 2.8 GHz is chosen simply because, such a source is commercially available in the form of a relativistic S-band magnetron [15].

frequency = 2.8 GHz wavelength = 0.107 m period = 357 ps

A. Available source

frequency = 2.8 GHz P_{peak} = 0.7 GW; pulse width = 40 ns

in WR-284 waveguide

This corresponds to a E_{peak} in WR-284 waveguide of 17.9 MV/m with 112 cycles in a single shot.

ELLIPTICAL REFLECTOR AT 1.1 GHz

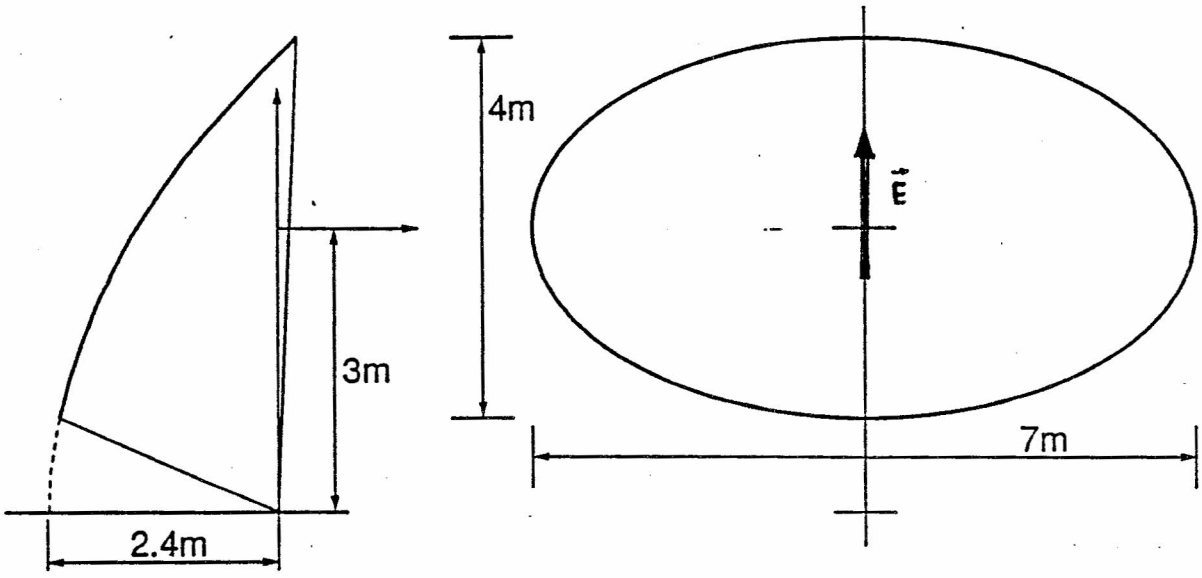

a) reflector geometry with an offset feed

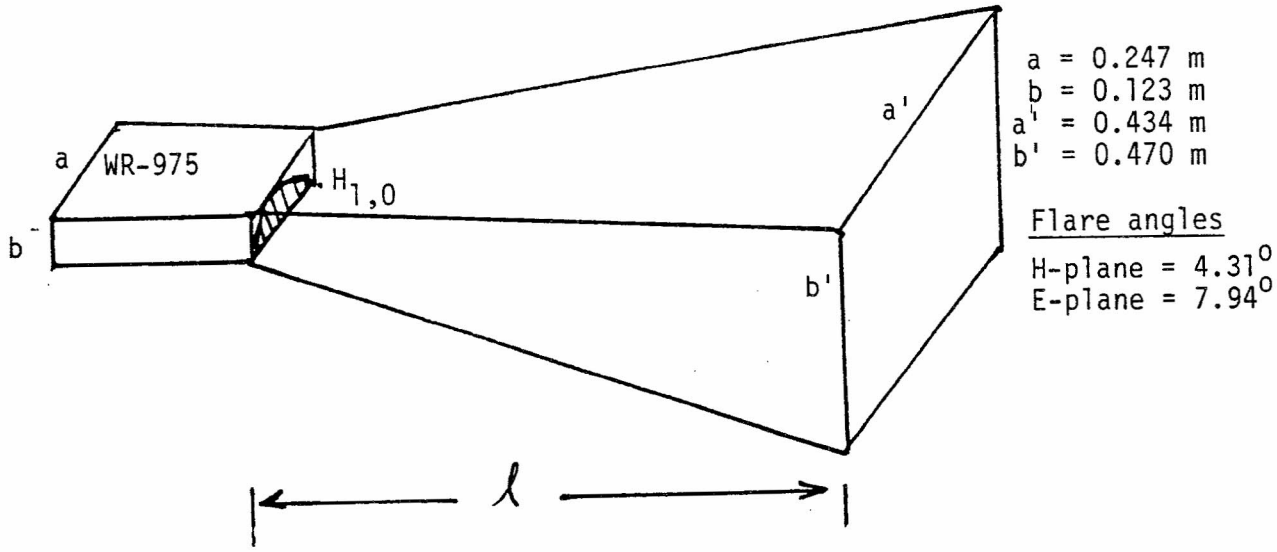

Figure 7. An offset fed elliptical reflector (examples)

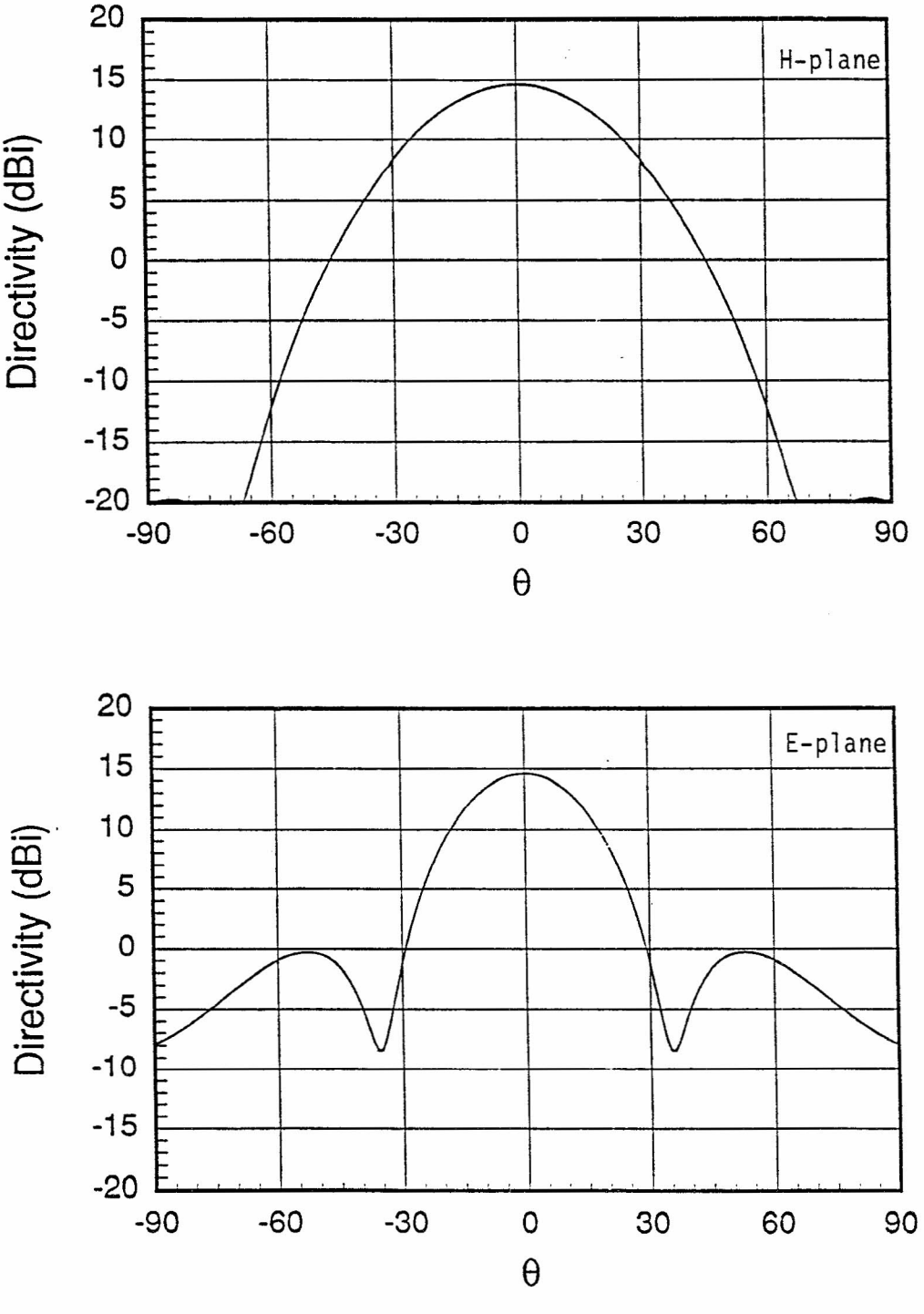

Figure 8. Radiation patterns of the pyramidal horn in figure 7.

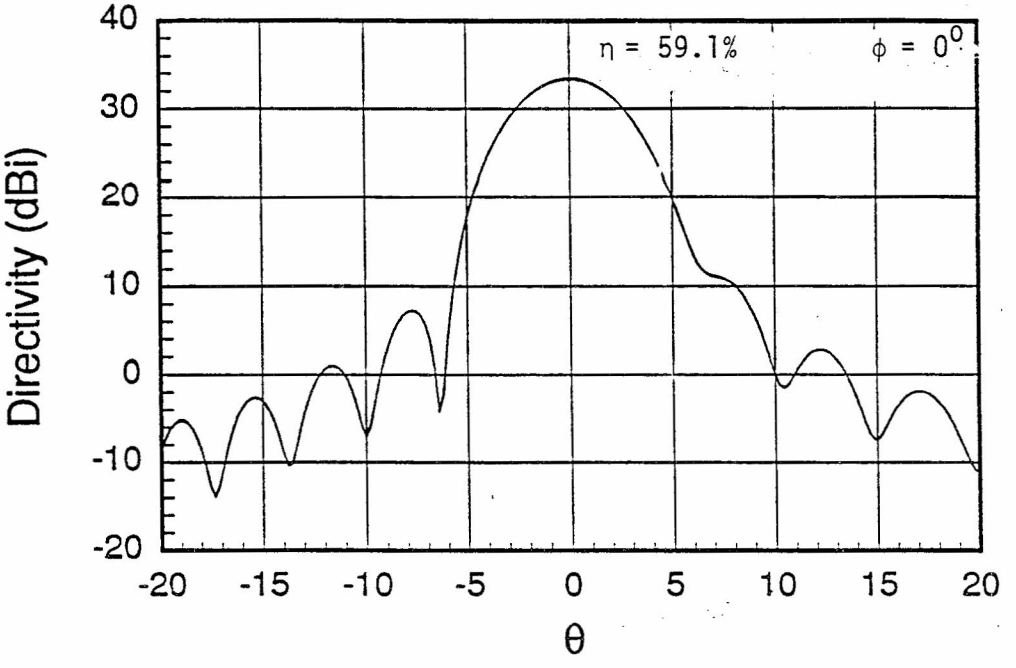

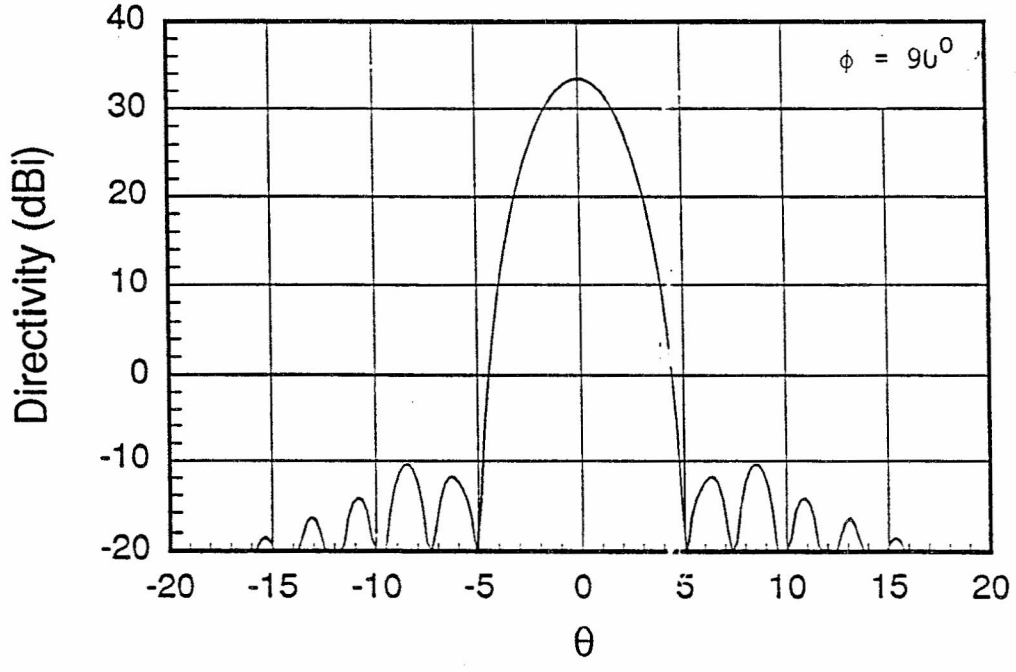

Figure 9. Radiation patterns of the elliptical reflector at 1.1 GHz.

B. Modified S-band source with a new waveguide extraction

frequency = 2.8 GHz; P_{peak} = 2 GW; pulse width = 40 ns

in WR 340 waveguide ($Z_{1,0}$ = 462.4Ω), containing 112 cycles.

This corresponds to a E_{peak} in the waveguide of 22.36 MV/m. The $H_{1,0}$ cut off frequency in WR-340 is 1.737 GHz and the next higher cut off is at 3.474 GHz which is about 24% over the operating frequency of 2.8 GHz. Although it is a significant jump from the available 0.7 GW to 2 GW power level, the 2 GW level appears feasible at this frequency. Suitable design changes may easily be done if this useful power level has to be revised downward.

C. Directional coupler

As before, design equations and curves in [16] may be used to fabricate the required ~90 dB side wall coupler(s).

D. Horn feed and dual reflector antenna

The design of a pyramidal horn and a dual reflector cassegrain antenna is available in [13] at a frequency of 3 GHz. Some dimensions of the waveguide and the horn are listed in Table 6.

TABLE 6. Some dimensions of the waveguide and feed horn

WR-340 waveguide	Pyramidal horn	
a = 86.36 mm	a' = 50.4 cm	
b = 43.18 mm	b' = 47.91 cm	f = 2.8 GHz
a/λ = 0.806	a'/λ = 4.7041	λ = 10.714 cm
b/λ = 0.403	b'/λ = 4.4718	NOTE: (a/a') = 0.171 (b/b') = 0.090
E_{peak} = 22.36 MV/m	E_{peak} (exit) = 2.78 MV/M	$\sqrt{\frac{ab}{a'b'}}$ = 0.124

The dual reflector antenna geometry, can be the same as indicated in figure 6 of [13], where the main reflector and subreflector dimensions are shown in terms of the wavelength (= 10.714 cm). In particular the subreflector diameter D_s is 10.2 λ = 109.28 cm, which means, roughly the peak field at the subreflector is given by

$$E_{peak}\,(\text{subreflector}) = E_{peak}\,(\text{waveguide}) \times \frac{b}{D_s} \simeq 880\ \text{kV/m}$$

which indicates that the subreflector is enclosed in the polyethelene bag that holds the SF_6 gas at 1 atmospheric pressure to provide additional safety margin. To a first order, the peak field at the main reflector will scale by the ratio fo the diameters of the two reflectors (D_s and D) resulting in a peak electric field of about 270 kV/m, since D = 33 λ and D_s = 10.2 λ resulting in D_s/D of about 0.31. Physical diameter and aperture area of main reflector in this example are 3.536 m and ~10 m^2.

Once again assuming a uniform illumination of the main reflector (not quite the case), one can estimate the far field, the average power density and the fluence using (10), (11) and (12). The far field characteristics for this Mark 0 Phaser at 2.8 GHz are listed in Table 7.

TABLE 7. Far field characteristics of Mark 0 Phaser at 2.8 GHz with 10 m^2 radiating aperture (illustrative example)

R km	E_{peak} (far field) kV/m	p_{avg} (far kW/m^2	fluence U J/m^2
0.3	84	9,358	3.743×10^{-1}
1	25.2	842	3.368×10^{-2}
3	8.4	93	3.720×10^{-3}
10	2.52	8.4	3.360×10^{-4}
30	0.84	0.93	3.720×10^{-5}

IV. Concluding Remarks

The effects of the far field parameters such as field strength and the fluence levels on electronic systems could be estimated as follows.

A. Field strengths

It was seen in Table 4 that a Mark 0 Phaser at a frequency of 1.1 GHz, can produce a field strength of 1.3 kV/m at a distance of 10 km. The pulse length was 100 ns, which contains about 110 cycles. If 110 cycles of microwave signals are incident on the target, it should be adequate to ring up the response to a level that a CW signal would. At this frequency of 1.1 GHz, the wavelength is 27.27 cm and an effective height of a near resonant antenna is about 10 cm. Assuming as matched load, say 50 Ω at the antenna terminals, the open circuit voltage is of the order of 130 V. This is indeed quite high and potentially result in an overvoltage breakdown of the receiver diode.

B. Fluence

It is reported in the literature that one class of electronic components most sensitive to microwave burnout are the microwave detector diodes, some of which have burn out thresholds of 1 μJ [17]. The energy contained in the voltage pulse estimated above is approximately,

$$\left[\frac{V^2}{R}\right] \times 100ns \simeq 33\,\mu J$$

However, it is not clear how much of this energy is deposited into the diode per se. The amount of energy deposited into the diode could be more or less than the energy in the voltage pulse, depending on the details of the circuit. The energy deposited in the diode could exceed the energy in the voltage pulse, if the power source biasing the diode adds to the voltage pulse. For this reason, the induced voltage across the diode is a quantity that is assuredly more damaging.

In addition to the above discussed "breakdown" or "burnout" types of damage, which are the result of front door coupling, one could also expect "bit-error" type of damage in unshielded computers via back door coupling. It is reported that "bit-error" damage is caused in unshielded computers in the fluence range of 10^{-4} to 10^{-3} J/m^2. Precisely, how much fluence is delivered to unprotected electronic instrumentation via back door coupling is a system specific issue and there are many factors governing this type of potential damage.

One may conclude however that even truck mountable systems with a 1 GW source have adequate field strengths at several km to potentially cause damage by both front and back door coupling mechanisms. It then becomes evident what a progression of such phasers can do in terms of damaging unprotected systems.

References

[1] C. E. Baum, Focused Aperture Antennas, Sensor and Simulation Note 306, May 1987.

[2] C. E. Baum, Maximization of Electromagnetic Response at a Distance, Sensor and Simulation Note 312, October 1988.

[3] C. E. Baum, A Rational Approach to the Development of a HPM Weapon, Microwave Memo 1, October 1988.

[4] C. E. Baum, The Phaser, Microwave Memo 2, November 1988.

[5] C. E. Baum, Some Features of Waveguide/Horn Design, Sensor and Simulation Note 314, November 1988, and Chap. 11.3, ppo. 480-497, in H. Kikuchi (ed.), *Environmental and Space Electromagnetics*, Springer Verlag, 1991.

[6] C. E. Baum, Combining RF Sources Using C_N Symmetry, Circuit and Electromagnetic System Design Note 37, June 1989.

[7] C. E. Baum, Matching Modulated Electron Beam to Waveguide, Circuit and Electromagnetic System Design Note 39, April 1990.

[8] D. V. Giri, Preliminary Considerations for High-Power Microwave (HPM) Radiating Systems, Circuit and Electromagnetic System Design Note 40, December 1990.

[9] D. V. Giri, Canonical Examples of High-Power Microwave (HPM) Radiation Systems for the Case of One Feeding Waveguide, Sensor and Simulation Note 326, April 1991.

[10] C. E. Baum, The Microwave-Oven Theorem: All Power to the Chicken, Microwave Memo 3, June 1991.

[11] C. E. Baum, Preliminary Near-Term Criterion for Single-Pulse HPm, Microwave Memo 4, July 1991.

[12] D. V. Giri and Y. Rahmat-Samii, Effects of Waveguide Dispersion on High-Power Microwave Signals, Sensor and Simulation Note 331, September 1991.

[13] Y. Rahmat-Samii, D. W. Duan, and D. V. Giri, Canonical Examples of Reflector Antennas for High Power Microwave Applications, Sensor and Simulation Note 334, October 1991.

[14] C. E. Baum and D. V. Giri, Mark N Phaser, Microwave Memo 5, 4 February 1992.

[15] J. Benford, Physics International Company, San Leandro, CA, Private Communication, February 1992.

[16] T. S. Saad, R. C. Hansen, and G. J. Wheeler (editors), Microwave Engineer's Handbook, Volume 2, pages 2 and 8, ArTech House, 1971.

[17] M. K. Florig, The Future Battefield : a blast of Gigawatts?, IEEE Spectrum, March 1988, pp. 50-54.